Cite this: DOI: 10.1039/c0xx00000x

www.rsc.org/xxxxxx

ARTICLE TYPE

Total oxidation of naphthalene at low temperatures using palladium nanoparticles supported on inorganic oxide-coated cordierite honeycomb monoliths

Francisco J. Varela-Gandía[a], Ángel Berenguer-Murcia[a], Dolores Lozano-Castelló[a], Diego Cazorla-Amorós[a*], David R. Sellick[b], Stuart H. Taylor[b*]

Received (in XXX, XXX) Xth XXXXXXXXX 20XX, Accepted Xth XXXXXXXXX 20XX
DOI: 10.1039/b000000x

A study on the preparation of thin films of ZSM-5 and BETA zeolites, and a SAPO-5 silicoaluminophosphate, supported on cordierite honeycomb monoliths by *in situ* synthesis was carried out for their use as catalyst supports. Furthermore γ-Al_2O_3 was also coated onto a cordierite honeycomb monolith by a dip-coating method for use as a standard support. Structured monolithic catalysts were prepared by impregnation of the aforementioned coated monoliths with polymer-protected Pd nanoparticles. The monolithic catalysts have been tested for the total oxidation of naphthalene (100 ppm, GHSV 1220 h^{-1}). From the combined use of the zeolite with polymer-protected nanoparticles, enhanced catalytic properties have been found for the total abatement of naphthalene. The Pd/MBETA and Pd/MZSM-5 catalytic monoliths have shown excellent activity with a high degree of stability, even after undergoing accelerated ageing experiments.

Introduction

Polycyclic aromatic hydrocarbons (PAHs), such as naphthalene, are environmentally hazardous compounds produced as a result of the incomplete combustion or pyrolysis of organic material [1-5]. Naphthalene is considered the least toxic and simplest molecule of the PAHs, and thus it is used as a model compound for this group of pollutants. In the literature, a range of different technologies have been studied to reduce PAH emissions [6-13]. Among them, catalytic combustion is the most promising for the removal of PAHs from polluted air streams, due to its lower operating temperature and higher selectivity towards CO_2 [2].

For catalytic total oxidation, the types of catalysts used are based to a large extent on metals such as Pd, Pt, Ru or Co supported on γ-alumina by impregnation [14], metal oxide catalysts [2,15-19], mesoporous aluminosilicates with supported Pt [20] or the use of zeolites ion-exchanged with Pt [21]. Based on our previous studies [22], the use of polymer protected Pd nanoparticles supported on zeolites is one of the most promising types of catalyst for the total oxidation of naphthalene, due to the low oxidation temperature reported (165-180ºC), and the high stability of the catalyst.

However, for practical applications macro-structured catalysts are preferred over powdered catalysts. For example, a monolithic reactor can involve a single block of material containing a large number of parallel channels, which are available in various sizes or shapes [23]. Low pressure drops, uniform flow distribution, absence of hot spots and good tolerance to plugging by dust are essential requisites that ultimately lead to the use of catalytic monoliths [23,24]. For gas phase applications, metal or ceramic honeycomb monoliths are standard support materials. In reference to ceramic monoliths, the support structure is made of a non-catalytic, thermally resistant material, typically cordierite, onto which a catalytic layer is deposited [25]. The chemical composition of the cordierite is based on $2MgO{\cdot}2Al_2O_3{\cdot}5SiO_2$ and a cordierite monolith has excellent operational properties such as low pressure drops in the exhaust system, good thermal resistance, refractoriness, good wash-coat adherence and compatibility between wash-coat and catalyst [26,27]. Concerning the deposition method for active phases, different strategies can be employed for initially coating the monolith channels with a support material, like alumina, silica, ceria and zeolites, followed by subsequent impregnation with an active phase [28]. In the case of zeolites or SAPO materials, there are two ways to coat the monoliths: hydrothermal synthesis using either direct synthesis or seeded growth, referred to as *in situ* synthesis, and dip-coating or wash-coating, which consists of deposition from a slurry of zeolite particles followed by a stabilizing thermal treatment [24].

In the present study, two different zeolites (BETA and ZSM-5) and a silicoaluminophosphate molecular sieve (SAPO-5) have been selected as coating materials for cordierite monoliths by *in situ* synthesis. Furthermore, a commercial γ-Al_2O_3 has been coated on the monolithic supports by the dip-coating method for comparative purposes. The active phase that will be employed is polymer protected Pd nanoparticles, which have shown good properties as catalysts for naphthalene total oxidation with the supports above, when they were used as powder catalysts [22]. Special attention has focused on the stability and recyclability of

the structured catalysts for extended time-on-stream experiments.

Experimental

Catalyst preparation

Coating monoliths with BETA, ZSM-5, and SAPO-5

Cylindrical cordierite monoliths (Corning) were used as supports (400 cpsi, length (l): 14 cm, diameter (d): 14 cm). These were cut into small cylindrical pieces (l: 1.6 cm, d: 1.4cm, mass: ~ 1.2 g). Prior to coating, all the small monoliths were blown with air to remove the dust produced in the cutting process. A calcination process in static air in a furnace at 800ºC for 2 hours (heating rate: 6 ºC/min) was performed with the aim to remove organic impurities.

The growth of BETA and ZSM-5 zeolites and SAPO-5 silicoaluminophosphate molecular sieve was carried out by *in-situ* synthesis onto the cordierite monolith avoiding the use of binders. The general experimental procedure for the synthesis of the zeolites and the silicoaluminophosphate onto the monolith was:

i. The cordierite honeycomb monoliths were wrapped with Teflon tape to prevent zeolite growth on the outer surface.
ii. The "teflonated" monoliths were placed in a stainless steel autoclave with a Teflon liner (V: 10 mL). A precursor gel/monolith weight ratio of 4 mL/g was used for coating the monoliths.
iii. The autoclaves were placed horizontally in a convection oven and rotated during the whole growth process (v = 4rpm) to ensure a homogeneous growth of the solid film and prevent blocking of the monolith channels [27]. Four monoliths were prepared per batch.
iv. The crystallization step was carried out at the desired temperature and time for each crystalline material.
v. After the hydrothermal synthesis, the autoclaves were submitted to "Fast cooling" using running tap water.
vi. After the synthetic protocol, the coated monoliths were washed with abundant quantities of distilled water and dried at 100 ºC overnight. All the monoliths were submitted to sonication for 6 hours to remove loosely adhered crystals and then, dried again overnight in an oven at 100 ºC.

Two consecutive synthesis steps were performed. Thus, after finishing the whole procedure described above the samples were again placed into an autoclave for a second synthesis process using a fresh synthesis solution (i.e. points (2) to (6) were repeated).

After preparing the coated monoliths using two consecutive syntheses, the removal of the template was carried out by calcination at the desired temperature for each material in a muffle furnace under static air (heating rate 1 ºC/min). Finally, the total weight increase for both the first coating step performed and the whole coating process was measured. The increase in mass is indicative of the loading and is expressed as wt%.

Coating of the monoliths with zeolite BETA was carried out following the methodology reported by Bueno-Lopez *et al.* [27], but it was adapted to our larger monolith size. The details of the molar compositions of the synthesis gel are given in [19]. The optimum conditions found for the synthesis of zeolite BETA on cordierite monoliths were two consecutive synthesis steps with a crystallization temperature of 132ºC for 48 hours. The BETA coated monoliths, named MBETA, were submitted to a calcination step to remove the template at 500 ºC for 6 hours.

ZSM-5 coated monoliths, which are called MZSM-5 in this work, were obtained after two consecutive synthesis steps. As mentioned previously by Ulla *et al.* [25], the coating of high aluminium content zeolites is hindered by Al-rich supports, such as cordierite, and therefore it is necessary to combine two synthesis protocols using materials with different Si/Al ratios. For this reason, the first-crystallization step was the preparation of a silicalite-1 coating, which is isostructural to ZSM-5, but with no aluminium content in its framework, in order to ensure the crystallization and anchoring of the ZSM-5 zeolite onto the monolith. Thus, the synthesis was performed adapting the methodology for the preparation of silicalite-1/carbon membranes reported by Berenguer-Murcia *et al.* [29]. The silicalite-1 solution was obtained by adding 3.420g of TEOS (tetraethoxysilane) dropwise into a 1M Tetrapropylammonium hydroxide TPA-OH solution (4.920 g TPA-OH solution, in 31.570 g of distilled water). The resulting solution was aged for 90 min and the monoliths were coated with a layer of silicalite-1 after a crystallization time of 6 hours at 180ºC. The second crystallization step consisted of the preparation of a ZSM-5 zeolite coating. The details of the experimental procedure used for the preparation of ZSM-5 zeolite are given in detail elsewhere [30]. According to reference [30], the crystallization conditions are 190ºC for 10 hours. Template removal was carried out by calcination in static air at 550 ºC for 4 hours.

SAPO-5 monoliths, named MSAPO-5, were prepared by adapting the procedure described by Campelo *et al*. [31] for the preparation of powdered SAPO-5. The crystallization was performed at 200ºC and crystallization times between 18 and 24 hours were used for studying the coating process. The calcination process for MSAPO-5 monoliths was performed at 600ºC for 6 hours.

Coating of γ-Al_2O_3

A coating of γ-Al_2O_3 onto selected honeycomb cordierite monoliths was performed by dip-coating and the samples were labeled as M-γ-Al_2O_3. Prior to the dip-coating step, the cordierite monoliths were wrapped with Teflon tape to avoid deposition of γ-Al_2O_3 on their outer surface. M-γ-Al_2O_3 monoliths were prepared following the procedure described by Villegas *et al.* [32]. Theγ-Al_2O_3 powder was dispersed in HNO_3 (γ-Al_2O_3/H_2O = 25 wt. %, HNO_3/ γ-Al_2O_3 = 2 mmol/g) using a high-shear mixer (ULTRA TURRAX T25, IKA Labortechnik). Initially, the required amount of γ-Al_2O_3 powder was added to the acid solution for 10 min at 7000 rpm. After vigorous stirring (14000 rpm) for 5 min at room temperature, the stable suspension was used for dip-coating. A series of 8 monoliths were prepared with each dip-coating suspension, in order to check the reproducibility of the coated monoliths. The monoliths were immersed vertically into the suspension for 2 minutes and the excess suspension was removed using a flow of compressed air. Finally, the monoliths were dried at room temperature for 24 hours whilst continuously rotating horizontally to ensure optimum coating distribution. The procedure was performed twice with a fresh suspension. M-γ-Al_2O_3 monoliths were calcined in static air at 600 ºC for 4 hours (heating rate 1 ºC/min).

Deposition of Pd nanoparticles

Palladium nanoparticles protected by polyvinylpirrolidone (PVP)

were synthesized by the reduction-by-solvent method as reported previously [33]. The catalysts used in this work were prepared by the impregnation method, as reported in our previous work for powdered catalysts [22]. The aforementioned coated monoliths were wrapped with Teflon tape in order to fix them vertically in 10 mL Teflon liners and to prevent deposition of Pd nanoparticles on the outer surface of the cordierite monolith. The required concentration of Pd nanoparticles, suspended in methanol, was added based on the total amount of BETA, ZSM-5, SAPO-5 or γ-Al_2O_3 coating, to yield a nominal 1wt.% of metallic loading with respect to the zeolite, SAPO-5 or Al_2O_3. To ensure the complete immersion of the coated monoliths in the suspension additional methanol was added to give a final volume of 5 ml. The Teflon liners filled with the monolith and Pd suspension were placed in a thermostated bath, stirred at 60 rpm at room temperature for two days. Subsequently, they were transferred to an oven, where they were left at 60 ºC in order to evaporate the solvent and obtain the final structured honeycomb monolith, labeled Pd/MBETA, Pd/MZSM-5, Pd/MSAPO-5 and Pd/Mγ-Al_2O_3.

Characterization of the catalysts

ZSM-5 and BETA zeolites and SAPO-5 silicoaluminophosphate molecular sieve supported on cordierite monoliths were characterised by XRD, using a 2002 Seifert powder diffractometer. The scanning rate was 2 º/min and Cu-Kα radiation was used.

The coated monoliths were characterized by SEM in a JEOL microscope (model JSM-80). The monoliths were carefully cut parallel to the monolith axis. This procedure allowed the analysis of the surface of the monolith channels, and the thickness and homogeneity of the coated layer. In the case of the Pd-containing catalysts, they were cut in the same manner and analyzed by SEM in a HITACHI S-3000 microscope. Energy-dispersive X-ray spectrometry (EDX) was used to ascertain the Pd concentration along the channels by careful cutting of the monolith along its length.

Textural characterization of the coated monoliths and the catalysts was carried out by means of adsorption of N_2 at -196 ºC (Autosorb 6, Quantachrome). Prior to the adsorption measurements, the samples were outgassed under vacuum (10^{-2} mbar) at 250 ºC for 4 h to remove any adsorbed impurities. Surface area was calculated from nitrogen adsorption isotherms using the BET equation (S_{BET}). Total microporevolumes (V_{DR} (N_2)) were calculated by applying the Dubinin-Radushkevich (DR) equation to the N_2 adsorption data at -196 ºC [34].

Catalyst performance

Catalytic activity tests for naphthalene oxidation were carried out in a fixed bed reactor (diameter =1.6 cm). The feed stream consisted, in all cases, of 100ppmv naphthalene in a mixture of 20% O_2 and 80% He. The total flow was set to 50ml/min (GHSV = 1220 h^{-1}). Analysis of reactants and reaction products was performed by on-line gas chromatography using thermal conductivity and flame ionization detectors. The catalytic activity was measured over the temperature range 100-200ºC in incremental steps and temperatures were measured by a thermocouple placed in the catalyst bed connected to a PID controller. Data were collected at each temperature after a stabilization time of 20 minutes. Three analyses were made at each temperature to ensure steady state was attained. Oxidation activity is expressed as a yield of carbon dioxide. Furthermore, accelerated time-on-line experiments for long-term use of these catalysts were performed with the aim to determine potential deactivation. For this purpose, the catalysts were submitted to reaction conditions at 250ºC for 48 hours.

Results and discussion

Coated monoliths characterization

Table 1 shows the percentage of weight increase on coated monoliths after the first and second coating steps. According to Bueno-Lopez *et al*. [27] in order to improve zeolite loading and deposit a thin and homogeneous zeolite layer, autoclave rotation during the hydrothermal treatment and a second synthesis step are necessary. It is worth mentioning that both the supported zeolite and SAPO-5 crystals (after the first step) and the zeolite and SAPO-5 layer (after the second step) are highly stable towards sonication, indicating good adhesion of the zeolite to the monoliths surface. Therefore, the error in the estimation of the weight increase after two coating steps is reasonably low, considering the complex process under study, including crystallization, cleaning and calcinations steps. M-γ-Al_2O_3 monoliths, prepared in batches of 8 monoliths at a time, possess a high reproducibility with a weight increase and standard deviation similar to observations by Villegas *et al.* [32].

Table 1 Monolith weight increase (wt%) for single and two steps coatings.

Coated monolith	First coating step (wt.%)	Second coating step (wt.%)
MBEA	3.6±0.4	17.7±2.0
MZSM-5	4.0±0.4	15.8±1.8
MSAPO-5	4.9±0.9	16.1±1.7
Mγ-Al_2O_3	9.4±1.4	15.0±1.7

X-ray diffraction was used to confirm the phase purity and crystallinity of the zeolite or SAPO layers coated on the cordierite monoliths after two synthesis steps. Figure 1 compiles the diffractograms of uncoated cordierite and coated monoliths (MBETA, MZSM-5 and MSAPO-5). Powder zeolites and SAPO-5diffractograms have been added to confirm the crystallinity of the coating layer; the diffractogram for the coated monoliths show the same characteristic peaks of the powdered zeolites (indicated by full dots on the corresponding peaks) [35]. Therefore, it can be confirmed that the crystallinity of the zeolites are maintained when they are supported on the monoliths.

In the case of MSAPO-5 monoliths, a synthesis time between 18-24h was used. From the analysis of the XRD of the samples prepared after 18, 20, 22 and 24h (results not shown), it was confirmed that only the MSAPO-5 prepared after 18h (XRD included in Figure 1) showed the characteristic peaks of the SAPO-5 silicoaluminophosphate (AFI structure) without the appearance of other crystalline phases. Consequently, all the monoliths synthesized for this work were prepared with a synthesis time of 18h.

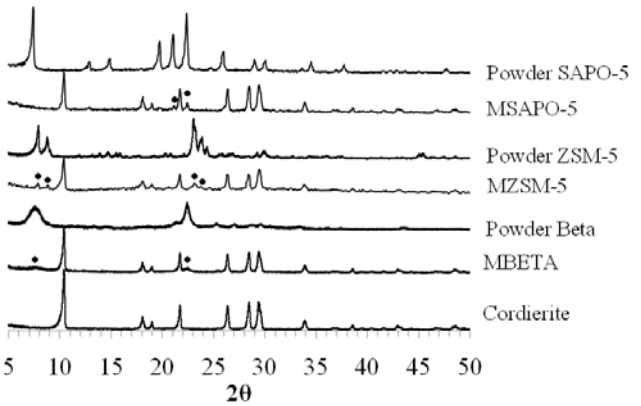

Fig. 1 XRD diffractograms of cordierite, coated monoliths and powder zeolites. The peaks corresponding to the zeolite phases are marked with full dots

Nitrogen adsorption was performed to analyze the porous texture of the as-prepared materials. From the nitrogen isotherms (see Figure 2) it is possible to confirm that cordierite exhibits negligible porosity; therefore, it can be assumed that there is no contribution of the cordierite support to the adsorption properties of the coated monoliths. Table 2 summarizes the surface areas (S_{BET}) and the total micropore volumes ($V_{DR}(N_2)$) calculated per unit weight of the monolith.

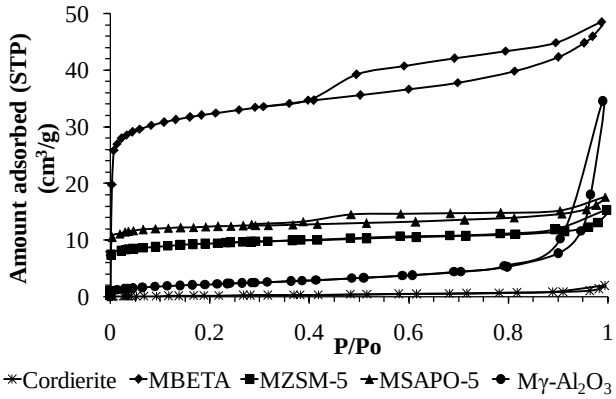

Fig. 2 Nitrogen adsorption/desorption isotherms at -196 °C

Table 2 Porous texture characterization results of the coated monoliths

Sample	S_{BET} (m^2/g)	V_{DR} (N_2) (cm^3/g)
Cordierite	1	0.00
MBETA	100	0.05
MZSM-5	35	0.02
MSAPO-5	35	0.02
Mγ-Al_2O_3	8	—[a]

[a] Not possible to determine.

In the case of Mγ-Al_2O_3 it presents a similar nitrogen adsorption isotherm as the powder γ-Al_2O_3 used to coat the monolith, which indicates that the dip-coating procedure used to prepare this sample does not modify significantly the porosity of the supported γ-Al_2O_3.

In reference to zeolite and SAPO coated materials, MBETA, MZSM-5 and MSAPO-5, the nitrogen adsorption isotherms also have the same shape, including the hysteresis loop, as the equivalent powdered samples prepared in previous work [35]. To compare the specific surface area (S_{BET}) area and micropore volume of the coated zeolites with the powdered zeolites, estimations for the monoliths have been made considering the weight of the zeolite coatings. These values have been excluded in this paper for brevity, but it is evident that both BETA and SAPO-5 layers have very similar porosity to the powder materials, thus practically they are unaffected by the *in situ* coating process.

On the other hand, the ZSM-5 layer, confirmed by X-ray diffraction, shows a lower porosity than the one expected from the comparison with a powder sample. The main reason is due to the coating procedure used for this sample. As we have mentioned previously, the coating of high aluminium content zeolites is hindered by Al-rich supports such as cordierite. According to Ulla *et al.* [25] the first step in the hydrothermal synthesis of zeolite films is the formation of a precursor gel layer onto the substrate, which serves as the primary source of nucleation. However, the addition of Al to the solution accelerates gel layer formation, but delays the nucleation and subsequent zeolite growth processes within it. Therefore, the use of Al-rich synthesis gels has a direct influence on the kinetics of the process and, as a consequence, high loadings of well-crystallized and anchored zeolite films are difficult to obtain. In a first synthesis, Silicalite-1 is used to provide a suitable environment for the growth of a high aluminium content zeolite in the second synthesis step. This first layer is partially dissolved during the second synthesis, helping the nucleation and growth of the second layer. Thus, this procedure may block or remove part of the first zeolite coating producing a reduction in the adsorption properties of the zeolite layer [36].

A detailed study of the different coated layers onto the cordierite monoliths was carried out by SEM. Figure 3 shows the original uncoated monolith. The top view shows that a cordierite monolith is a continuous support with macroscopic openings along the entire surface that will be accessible during the zeolite coating process. From the cross sectional view it can be established that the monolith walls are 150 µm wide and have a macroporous character.

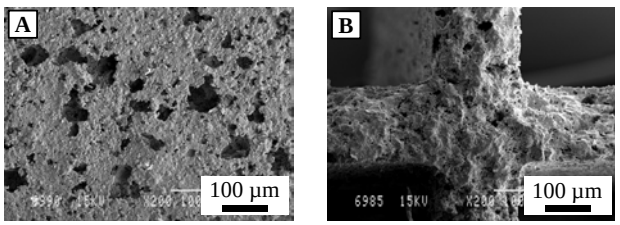

Fig. 3 SEM images of original uncoated cordierite honeycomb monolith (a) top view and (b) cross sectional view

Figure 4 shows the top view of the coated monoliths with BETA, ZSM-5, SAPO-5 and γ-Al_2O_3, respectively. After the first synthesis step (See Figure 4, left column), MBETA, MZSM-5 and MSAPO-5 monoliths have crystals which do not cover all the surface of the monoliths and, therefore, do not form a continuous layer. These individual crystals, however will act as seeds for the second *in-situ* synthesis step performed. The individual crystals formed onto the cordierite monoliths present the typical morphology for each type of zeolite, as has been reported in the literature for BETA [27,35], ZSM-5 [29,35] and SAPO-5 [37,38]. In reference to the Mγ-Al_2O_3, the slurry for dip-coating partially

covered the surface of the monoliths filling the external openings of the cordierite monoliths.

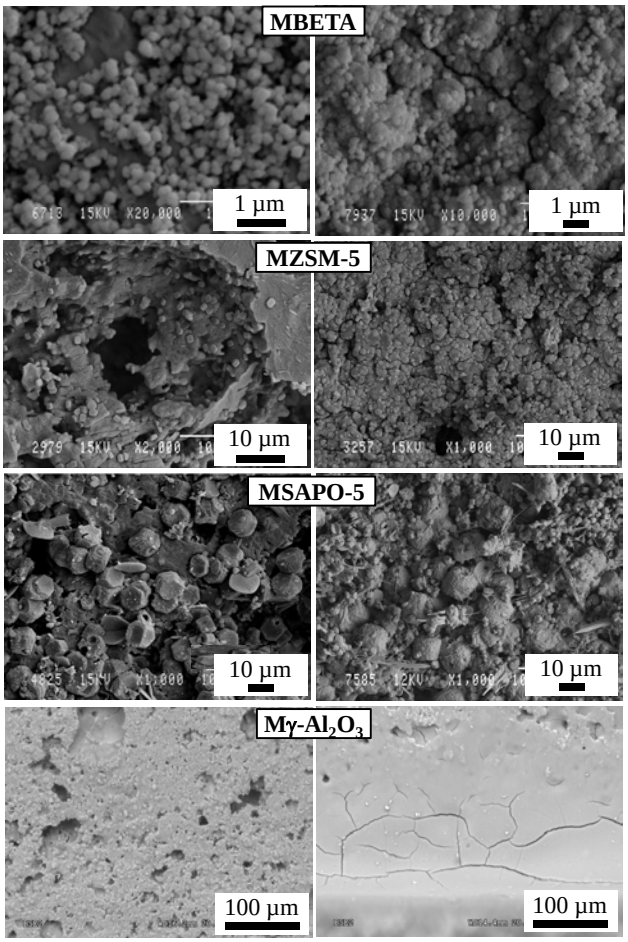

Fig. 4 SEM top view images for the four prepared monoliths after the first coating step (left column) and the second coating step (right column)

When a second synthesis step was performed (See Figure 4 right column), it is possible to cover all the surface of the monolith with a complete and homogeneous layer of intergrown crystals. MBETA and MZSM-5 crystals maintained their respective shape. It must be pointed out that the MSAPO-5 monolith presents a bimodal particle size distribution. The crystals appearing after the first synthesis have increased in size up to approximately 12 µm, and small SAPO-5 crystals have grown (approximately 1 µm), filling the gaps between the larger crystals, giving rise to a continuous layer. Finally, the Mγ-Al_2O_3 monolith prepared by the "dip-coating" method is formed by a homogeneous and continuous layer of Mγ-Al_2O_3 over the entire monolith wall. In spite of the deposited monolith coating layer being homogeneous, a significant quantity of γ-Al_2O_3 was preferentially deposited on the corners towards the centre of the channels, and small cracks were observed after the calcination step.

With the aim to analyze the thickness of the coated layer onto the monolith walls, SEM images of the cross sectional view are useful for this purpose (see Figure 5). All samples in this study prepared by the *in situ* synthesis method showed multiple layers of zeolite crystals. There were no significant differences between the coating zeolite or SAPO-5 layer in the centre and in the channel open ends, as well as along the channels, indicating that the movement of the autoclaves during synthesis results in a homogeneous growth along the channel length.

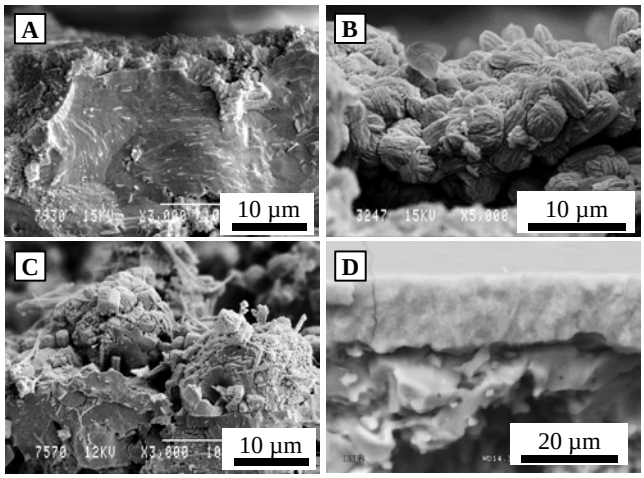

Fig. 5 SEM cross sectional images for the four prepared monoliths after the second coating step. (a) Sample MBETA, (b) Sample MZSM-5, (c) Sample MSAPO-5, and (d) Sample Mγ-Al_2O_3

Detailed analysis of SEM images has allowed us to conclude that the MBETA monolith (Figure 5a) is formed by a layer of intergrown zeolite crystals with an average thickness of 3 µm. Furthermore, the small crystal size of BETA zeolite permitted access to the internal openings of the monolith walls, thus giving rise to a zeolite deposit formed by the intergrowth between the crystals in the internal and external surface, producing a three dimensional network of the zeolite layer that results in high mechanical stability [27]. Figure 6 shows, as an example, a cross sectional view of a monolith wall, where the BETA zeolite layer was deposited on the cordierite wall, together with an internal opening filled with zeolite crystals.

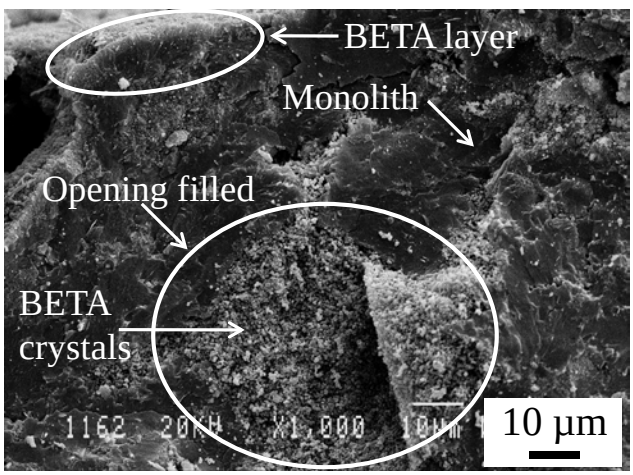

Fig. 6 SEM cross sectional images for BETA zeolite monolith with an internal opening completely filled with BETA zeolite

In the case of MZSM-5 monoliths, the coating layer consists of intergrown crystals with an average thickness of 6 µm. It is worth mentioning that the previous Silicalite-1 crystals deposited during the first synthesis cannot be observed. As explained previously, these crystals act as seeds for the deposition of a stable ZSM-5 layer and are partially dissolved during hydrothermal synthesis. MSAPO-5 monoliths are formed by a coated layer of intergrown

crystals with a bimodal particle size distribution with a layer thickness of around 12 µm. To conclude, for the monoliths prepared by *in situ* synthesis, it is important to note that MZSM-5 and MSAPO-5 only exhibit the crystallization of individual zeolite crystals in the internal openings without filling the porosity within the monolith walls, contrary to the behaviour observed for the MBETA monolith.

Analyzing the γ-Al_2O_3 layer on Mγ-Al_2O_3 monoliths (See Figure 5), a variation in thickness has been found. The thickness of the alumina wash-coating varies from 3-6 µm on the left side of the monolith to 16 µm on the other end of the opening, whilst it was about 12 µm in the middle of the channel as determined by SEM. This behaviour can be attributed to the immersion/extraction rate of the monolith from the slurry and the final step of blowing with air that may alter the coated layer at one of the ends.

Monolithic catalysts characterization

After impregnation, the monolithic catalysts were analyzed by XRD and no appreciable changes were observed in the prepared catalysts (results not shown).To analyze the distribution and loading of Pd nanoparticles on the monolith, Energy-dispersive X-ray spectrometry (EDX) was used to measure the quantity of Pd along the channels of the monolith. From the individual analysis performed on the four catalysts (Pd/MBETA, Pd/MZSM-5, Pd/SAPO-5 and Pd/Mγ-Al_2O_3), the general conclusion was that the amount of Pd in all the monoliths was around 1wt% with respect to the coating layer and the Pd was uniformly distributed along the channels.

Nitrogen adsorption was performed on the Pd-monolith catalysts in the same manner as the coated monoliths. Table 3 includes the BET surface areas (S_{BET}) and the total micropore volumes ($V_{DR}(N_2)$). Comparing the results with those obtained for the coated monoliths (see Table 2), it can be established that the catalyst preparation method has affected the adsorption properties of the coated layer on the Pd/MBETA and Pd/MZSM-5 and Pd/Mγ-Al_2O_3 only to a minor extent. Only in the case of the Pd/MSAPO-5 catalyst was there a significant reduction of the N_2 adsorption capacity compared to the MSAPO-5 monolith before impregnation with Pd nanoparticles. From the N_2 adsorption isotherms (results not shown), it is possible to confirm that, after impregnation with the Pd-based nanoparticles, the shape of the isotherms is the same as for the coated monoliths.

Table 3 Porous texture characterization results of the catalytic monoliths

Sample	S_{BET} (m^2/g)	V_{DR} (N_2) (cm^3/g)
Pd/MBETA	95	0.05
Pd/MZSM-5	35	0.02
Pd/MSAPO-5	10	—[a]
Pd/Mγ-Al_2O_3	7	—[a]

[a] Not possible to determine.

Comparing these results with powder catalysts Pd/BETA and Pd/ZSM-5 prepared previously, [22], the decrease in S_{BET} is lower in the coated monoliths. This behavior could be tentatively assigned to the location of deposited Pd nanoparticles. When a powder catalyst is prepared, the Pd nanoparticles are located over all of the zeolite crystals homogeneously. On the contrary, Pd nanoparticles in the coated monolith are predominantly distributed on the surface of the coating layer, due to the highly dense and compacted layers formed, as corroborated by EDX. Similar to the Pd/SAPO-5 powdered catalyst [22], the catalytic monolith shows the same decrease in apparent surface area.

As mentioned in our previous work [22], the synthesized Pd colloid shows very low polydispersity with a particle size of 1.8 ± 0.3 nm. In the case of the prepared monoliths it is not possible to observe the Pd dispersion using TEM, but deposition of polymer protected Pd nanoparticles did result in a noticeable change of Pd particle size according to our previous studies [22,33], so it is expected that the particle size increases when the polymer protected Pd nanoparticles are supported onto the coated monolith.

Catalytic performance in the oxidation of naphthalene

The catalytic activity of naphthalene oxidation was measured for the four monolithic catalysts. Three reaction cycles were performed with each catalyst in order to ensure the stability of the catalysts. This was achieved by incrementally increasing the reaction temperature to the desired set point and then cooling down to room temperature in order to start the next catalytic cycle. Additionally, it is noteworthy that no CO was detected as a reaction product in any of the experiments performed. Previous to testing the monolithic Pd catalysts, the coated monoliths (MBETA, MZSM-5, MSAPO-5 and Mγ-Al_2O_3) were tested in the oxidation of naphthalene and, in general, none of the coated monoliths was active at the temperature range studied (i.e. between 100 and 200 ºC). For example, the MBETA monolith was active at temperatures above 300 ºC reaching a 45% conversion of naphthalene to CO_2 at 350 ºC.

Figure 7 shows the variation of the catalytic activity (expressed as conversion towards CO_2) for naphthalene oxidation, as a function of the reaction temperature for the four Pd-monolith catalysts. After the first cycle, outstanding catalytic performance has been observed for the Pd/Mγ-Al_2O_3 and Pd/MSAPO-5 catalysts, whilst Pd/MZSM-5 and Pd/MBETA were able to reach full naphthalene conversion at higher temperatures. It is worth mentioning that the catalytic activity remained unchanged after three cycles, maintaining high naphthalene oxidation activity to CO_2 without any evidence for catalyst deactivation.

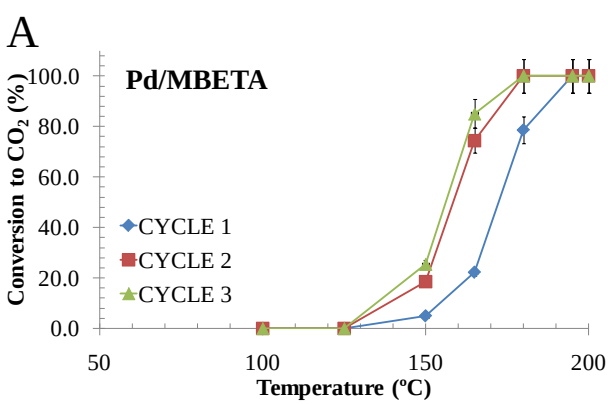

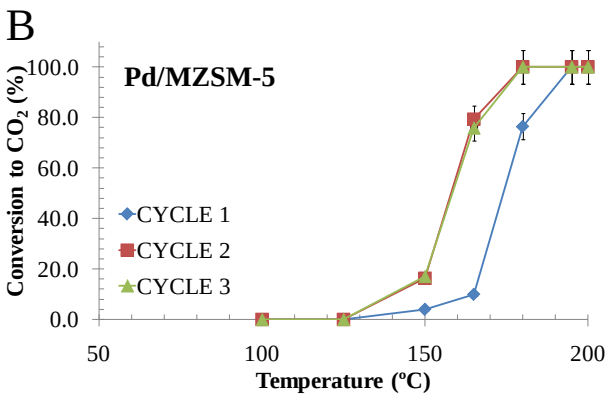

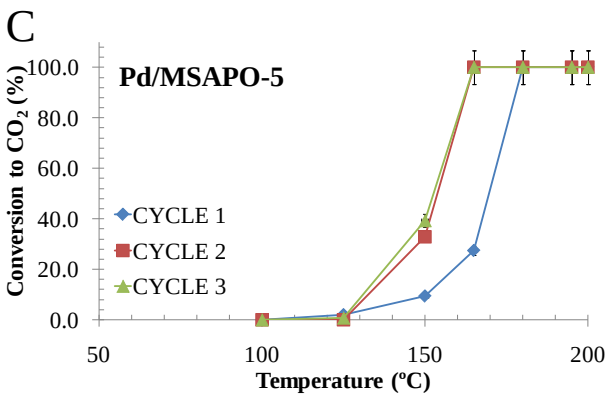

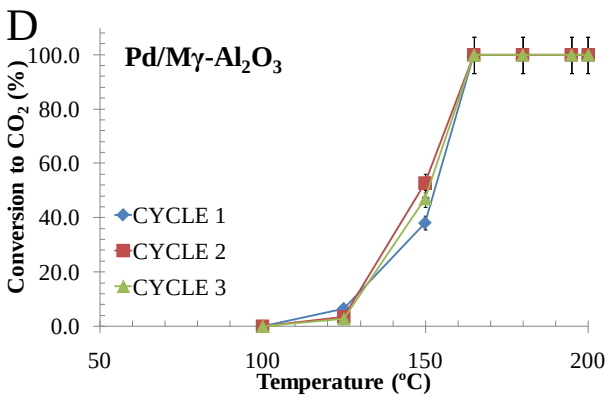

Fig. 7 Variation of the catalytic activity for naphthalene total oxidation (expressed as yield to CO_2) as a function of reaction temperature over the four catalysts. (a) Pd/MBETA, (b) Pd/MZSM-5, (c) Pd/MSAPO-5, and (d) Pd/Mγ-Al_2O_3

Table 4 shows the temperature required for total naphthalene oxidation to CO_2 for each monolithic catalyst over the three cycles studied. Comparing these results with our previous work [14] a small increase in the temperature needed to reach total oxidation is observed for the zeolite-coated monolith (BETA and ZSM-5). This can be due to the dense thin layer of the zeolite that may have an influence in naphthalene adsorption/desorption, thus having some effect on the kinetics of the process. Analyzing the CO_2 conversion at 150ºC in the monolith samples (see Table 5) and comparing with our previous work [22], the catalytic activity of the monoliths at 150 ºC shows a similar trend. The zeolite catalyst showed an increase of activity from the first to the third cycle, whilst the Pd/MAl_2O_3 showed reduced activity after three cycles. The activity is slightly lower for the catalysts in monolith form with respect to the powder form is slightly lower, and this is most probably due to increased diffusion limitations with the monoliths. Nevertheless, these are minor differences that show that the catalyst based on Pd nanoparticles supported on the coated-monoliths have a similar activity to the powder catalysts [22].

Table 4 Temperature required for naphthalene total oxidation for the different catalysts for the three oxidation cycles tested.

	Temperature (ºC) for total conversion to CO_2		
Catalyst	*Cycle 1*	*Cycle 2*	*Cycle 3*
1%Pd/MBETA	195	180	180
1%Pd/MZSM-5	195	180	180
1%Pd/MSAPO-5	180	165	165
1%Pd/Mγ-Al_2O_3	165	165	165

It is also useful to start to probe the stability of the active catalysts. An accelerated experiment to study possible deactivation as a function of time was conducted at 250ºC for 48h. Figure 8 shows the time-on-line data for the four Pd-monolith catalysts. It was evident that the Pd/MBETA and Pd/ZSM-5 samples were stable for at least 48h and there is no evidence of catalyst deactivation over the testing period. The yield of CO_2 at the beginning of the experiment was 100% and it was not diminished after 48h. Contrary to these two catalysts, Pd/MSAPO-5 and Pd/Mγ-Al_2O_3 exhibit a conversion of 100% during the first hours, but their conversion to CO_2 dropped to 92% and 90% for Pd/MSAPO-5 and Pd/Mγ-Al_2O_3, respectively, indicating possible deactivation, probably induced by the agglomeration of the Pd nanoparticles. Therefore, Pd/MBETA and Pd/MZSM-5 are the most suitable catalysts for naphthalene removal. In these cases, the rugosity of the prepared zeolite layer prevents the agglomeration of the Pd nanoparticles. These observations are in agreement with those for the powder catalyst [22].

Table 5 CO_2 conversion at 150ºC for the four catalysts and during the three cycles tested

	CO_2 conversion (%) (T=150ºC)		
Catalyst	*Cycle 1*	*Cycle 2*	*Cycle 3*
1%Pd/MBETA	5	19	25
1%Pd/MZSM-5	4	16	17
1%Pd/MSAPO-5	9	33	39
1%Pd/Mγ-Al_2O_3	38	53	43

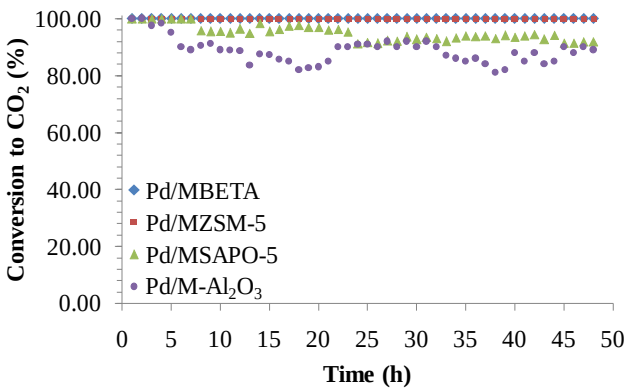

Fig. 8 Conversion of naphthalene to CO_2 as a function of time-on-line at 250ºC for the four monolithic catalysts

These results help to assess the viability of the monolith-based catalysts for naphthalene removal by catalytic oxidation, but a critical comparison with monolith-based catalysts from the literature should also be considered. Neyestenaki *et al.* [21] deposited ZSM-5 on cordierite monolith substrates by means of a ball-milled zeolite-water slurry method (monolith characteristics 400 cpsi, d=21.8 mm, h=20 mm), by dip-coating and drying several times, until a wash-coated loading between 13.5 and 30.8% and Pd, loaded by classical methods, was achieved. All the monolithic catalysts were tested for the removal of the emissions of pollutants from the combustion of biofuels in a simulated mixture, which contained naphthalene (50ppm), methane, CO, CO_2 and O_2, with a balance of N_2 (GHSV = 20000 h^{-1}). As expected, an increase in wash-coating loading resulted in decreased light-off temperatures of all the pollutants. Focusing on the monolith with similar characteristics (0.95%Pd/NaZSM-5) to our monolithic catalyst, the T_{50} was 246ºC and 243ºC for coated monoliths with an amount of ZSM-5 of 14.6%wt and 24.3%wt, respectively.

Ferrandon *et al.* [39] studied the total oxidation of mixtures with different concentrations of the same aforementioned pollutants, including 50 ppm of naphthalene (GHSV = 23000 h^{-1}, catalyst volume 6.5 ml). The monoliths used were composed of cordierite honeycomb monoliths (400 cps) wash-coated with γ-Al_2O_3 and used as supports for noble metal catalysts (Pd or Pt, 0.1mol%), metal oxides (MnO_xCuO_x,10 mol%) and combinations of noble metals with metal oxides. Analyzing the T_{50} temperature for the fresh monolithic catalyst, the Pd based catalyst was the most active (T_{50} = 200 ºC), whilst the metal oxides alone, MnO_x and CuO_x, were able to reach a conversion of 50% at 365 and 420 ºC, respectively. It was pointed out that impregnation of the metal oxides with Pd or Pt significantly decreased T_{50} for the resulting catalysts, however, they are still higher than those obtained in this study at least by 50 ºC. To conclude, all our monolithic catalysts show T_{50}values around 150-160 ºC after 3 cycles, indicating the benefits of the use of PVP polymer protected nanoparticles with more controllable properties. Furthermore, in our studies total oxidation of naphthalene is reached at lower temperatures.

Concerning the zeolite coated monoliths, a synergistic effect between using zeolites (BETA or ZSM-5) prepared by an *in situ* methodology with PVP-Pd nanoparticles, has been found. The catalytic monoliths are able to produce total oxidation of naphthalene at low temperatures, together with naphthalene removal from the gas stream by adsorption at lower temperature where the nanoparticles are not yet active. Secondly, the time-on-line experiments have identified that the catalysts are stable and thus should be regarded as suitable for the total oxidation of naphthalene in a practical application.

Conclusions

Zeolites BETA and ZSM-5, and silicoaluminophosphate molecular sieve, SAPO-5 have been coated on cordierite honeycomb monoliths (400 cpsi) by an *in situ* synthesis method. Two synthesis steps were required in order to coat the cordierite monoliths. The amount of zeolite introduced during the first single-step synthesis cannot completely cover the monolith surface, but it is used to seed the second synthesis step, which produces homogeneous and continuous thin zeolite films. Furthermore, the BETA coating layer is formed by a compact three-dimensional zeolite network conferring strong zeolite anchoring to the cordierite structure. In general, the preparation reproducibility of the coated materials was very high.

All the coated monoliths were impregnated with Pd-PVP-protected nanoparticles and were used as catalysts for the total oxidation of naphthalene. All the catalysts showed high activity for naphthalene conversion to CO_2, with total conversion taking place at 165 ºC after three cycles for Pd/MSAPO-5 and Pd/Mγ-Al_2O_3 and 180 ºC for Pd/MBETA and MSAPO-5 monoliths. All the catalysts possess high stability to temperature cycling, because their catalytic activity remained unchanged after testing for several oxidation cycles. Time-on-line experiments have been used to test the stability of the catalysts. The Pd/MBETA and Pd/MZSM-5 samples were stable after accelerated ageing time-on-line for 48 h at 250ºC. However, despite being the most active after three cycles, Pd/SAPO-5 and Pd/Mγ-Al_2O_3, exhibited decreased catalytic activity for the conversion of naphthalene to 95%, due to possible deactivation after ageing. It has been established that the use of Pd-based nanoparticles supported on BETA and ZSM-5 zeolites supported on honeycomb monoliths are very interesting options for the abatement of PAHs by catalytic oxidation.

Acknowledgements

The authors would like to thank the Spanish Ministerio de Ciencia e Innovación, Generalitat Valenciana, and FEDER (Projects CTQ2012-31762 and PROMETEO/2009/047) for financial support. F.J. Varela-Gandía thanks the University of Alicante for a PhD studentship. Á. Berenguer-Murcia thanks the Spanish Ministry for Economy and Competitiveness for a Ramón y Cajal fellowship (RyC 2009-03913).

Notes and references

[a] *Departamento de Química Inorgánica e Instituto Universitario de Materiales, Universidad de Alicante, Ap. 99, E-03080, Alicante, Spain. Fax: +34 96590 3454; Tel: +34 96590 3946; E-mail: cazorla@ua.es*
[b] *Cardiff Catalysis Institute, School of Chemistry, Cardiff University, Main Building, Park Place, Cardiff CF10 3AT, UK. Fax: +44 29208 74030; Tel: +44 29208 74062; E-mail: TaylorSH@Cardiff.ac.uk*

1 T. Garcia, B. Solsona, D. Cazorla-Amorós, Á. Linares-Solano, and S. H. Taylor, *Appl. Catal. B*, 2006, **62,** 66
2 B. Puertolas, B. Solsona, S. Agouram, R. Murillo, A.M. Mastral, A. Aranda, S.H. Taylor, and T. Garcia, *Appl. Catal. B*, 2010, **93**, 395
3 A.M. Mastral, and M.S. Callen, *Environ. Sci. Technol.*, 2000, **34**, 3051
4 A. Aranda, S. Agouram, J.M. López, A.M. Mastral, D.R. Sellick, B. Solsona, S.H. Taylor, T.García, *Appl. Catal.B*, 2012, **127**, 77.
5 S. Scirèa, L.F. Liotta, *Appl. Catal.B*, 2012, **125**, 222.
6 Z. Rui, Y. Lu, H. Ji, RSC Advances, 2013, **3**, 1103.
7 C.L. Lin, Y.H. Cheng, J.Y. Chen, *Journal of Hazardous Materials*, 2011, **197,** 254.
8 E. Ntainjua N., and S.H. Taylor, *Top. Catal.*, 2009, **52**, 528
9 C.C. Chang, C.Y. Chiu, C.Y. Chang, C.F. Chang, Y.H. Chen, D.R. Ji, Y.H. Yu, and P.C. Chiang, J. Haz. Mater., 161 (2009) 287-293.
10 L. Yu, X. Li, X. Tu, Y. Wang, S. Lu, and J. Yan, *J. Phys. Chem. A*,2010, **114**, 360.
11 M.H. Yuan, Y.Y. Lin, C.Y. Chang, C.C. Chang, J.L. Shie, and C.H. Wu, *IEEE Trans. Plasma Sci.*, 2011, **39**, 1092.

12 S.C. Marie-Rose, T. Belin, J. Mijoin, E. Fiani, M. Taralunga, F. Nicol, X. Chaucherie, and P. Magnoux, *Appl. Catal. B*, 2009, **90**, 489.
13 A. Bampenrat, V. Meeyoo, B. Kitiyanan, P. Rangsunvigit, and T. Rirksomboon, *Catal. Commun.*, 2008, **9**, 2349
14 X. Zhang, S. Shen, L.E. Yu, S. Kawi, K. Hidajat, and K.Y. Simon Ng, *Appl. Catal. A*, 2003, **250**, 341
15 T. Garcia, B. Solsona, and S.H. Taylor, *Appl. Catal.B*, 2006, **66**, 92
16 A. Aranda, E. Aylón, B. Solsona, R. Murillo, A.M. Mastral, D.R. Sellick, S. Agouram, T. García, S.H. Taylor, *Chem. Commun.*, 2012, **48**, 4704.
17 L. Torrente-Murciano, A. Gilbank, B. Puertolas, T. García, B. Solsona, D. Chadwick, *Appl. Catal.B*, 2013, **132-133,** 116.
18 D.R. Sellick, A. Aranda, T. García, J.M. López, B. Solsona, A.M. Mastral, D.J. Morgan, A.F. Carley, S.H. Taylor, *Appl. Catal.B*, 2013, **132-133**, 98.
19 T. Garcia, D. Sellick, F. Varela, I. Vázquez, A. Dejoz, S. Agouram, S.H. Taylor, B. Solsona, *Appl. Catal. A*, 2013,**450**, 169
20 J.-I. Park, J.-K.Lee, J. Miyawaki, W.-W.Pang, S.-H. Yoon, and I. Mochida, *Catal. Commun.*, 2010, **11**, 1068
21 A. K. Neyestanaki, L.-E Lindfors, T. Ollonqvist, and J. Väyryen, *Appl. Catal. A*, 2000, **196**, 233
22 F.J. Varela-Gandía, Á. Berenguer-Murcia, D. Lozano-Castelló, D. Cazorla-Amorós, David R. Sellick, and Stuart H. Taylor, *App. Catal. B*, 2013, **129**, 98
23 O. Öhrman, J. Hedlund, and J. Sterte, *Appl. Catal. A*, 2004, **270**, 193
24 J.M. Zamaro, M.A. Ulla, and E.E. Miró, *Chem. Eng. J.*, 2005, **106**, 25
25 M.A. Ulla, R. Mallada, J. Coronas, L. Gutierrez, E. Miró, and J. Santamaría, *Appl. Catal. A*, 2003, **253**, 257
26 Jimmie L. Williams, *Catal. Today*, 2011, **69**, 3
27 A. Bueno-Lopez, D. Lozano-Castelló, I. Such-Basáñez, J.M. García-Cortés, M.J. Illán-Gómez, and C. Salinas-Marinez de Lecea, *Appl. Catal. B*, 2005, **58**, 1
28 T.A. Nijhuis, A.E.W. Beers, T. Vergunst, I.Hoek, F. Kapteijn, and J.A. Moulijn, *Catal. Rev.*, 2001, **43**, 345380
29 Á Berenguer-Murcia, J. García-Martínez, D Cazorla-Amorós, Á Linares-Solano, and A.B. Fuertes, *Micropor. Mesopor. Mater.*, 2003, **59**, 147
30 H. Lechert, R. Kleinwort, and H. Robson (Eds.), *Verified Synthesis of Zeolitic Materials, 2nd ed.*, Elsevier, Amsterdam, 2001, pp. 198-200.
31 J.M. Campelo, F. Lafont, and J.M. Marinas, *J. Catal.*, 1995, **156**, 11
32 L. Villegas, F. Masset, and N. Guilhaume, *Appl. Catal. A*, 2007, **320**, 43
33 I. Miguel-García, Á. Berenguer-Murcia, and D. Cazorla-Amorós, *Appl. Catal. B*, 2010, **98**, 161
34 D. Lozano-Castelló, F. Suárez-García, D. Cazorla-Amorós, Á. Linares-Solano, in: F. Beguin, E. Frackowiak (Eds),*Carbon Materials for Electrochemical Energy Storage Systems*, CRC Press, Boca Raton (US), 2010, pp. 115-162.
35 J.M. López, M.V. Navarro, T. García, R. Murillo, A.M. Mastral, F.J. Varela-Gandía, D. Lozano-Castelló, A. Bueno-López, and D. Cazorla-Amorós, *Micropor. Mesopor. Mater.*, 2010, **130**, 239
36 V. Valtchev, J. Hedlund, B.J. Schoeman, J. Sterte, and S. Mintova, *Micropor. Mater.*, 1997, **8**, 93
37 J.M. Campelo, F. Lafont, J.M. Marinas, and M. Ojeda, *Appl. Catal. A*, 2000, **192**, 85
38 J.M. Campelo, F. Lafont, and J.M. Marinas, *Zeolites*, 1995, **15**, 97
39 M. Ferrandon, J. Carnö, S. Järås, and E. Björnbom, *Appl. Catal.A*, 1999, **180**, 153